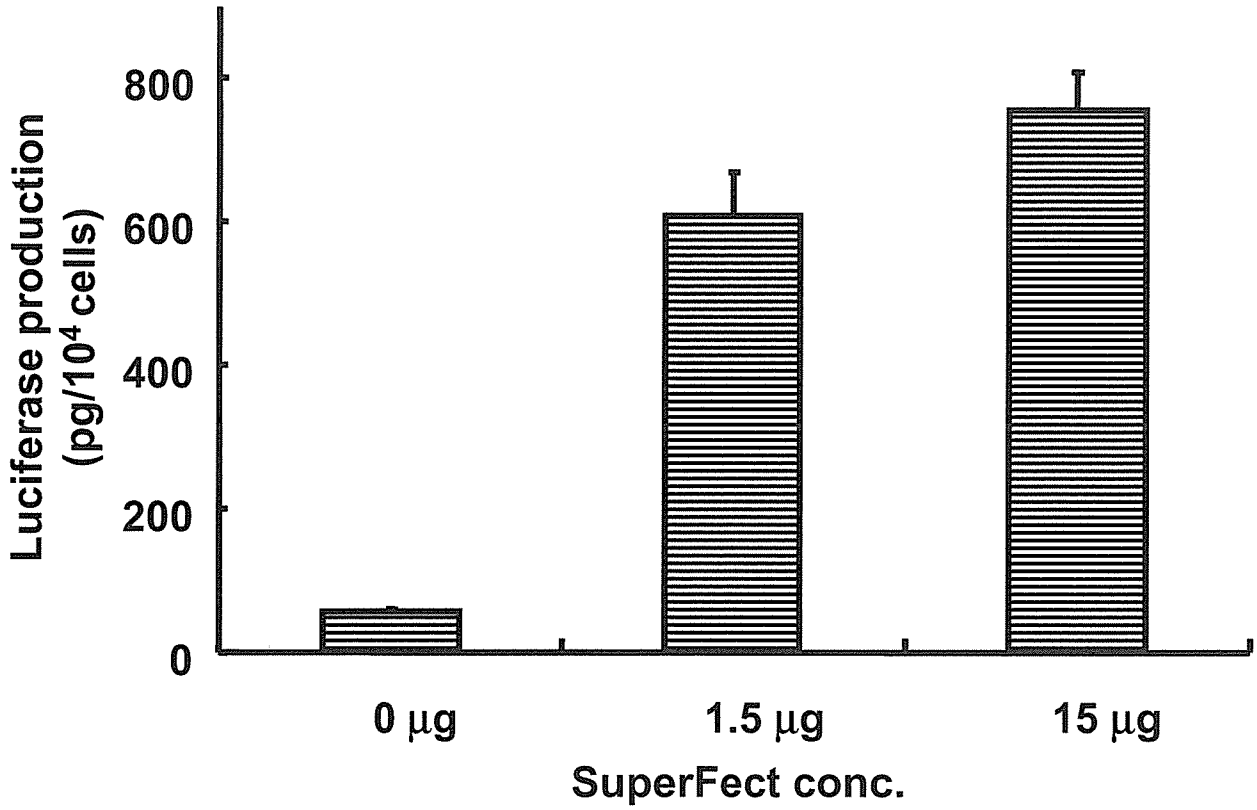

Fig. 56 Comparison of luciferase production in SK HEP-1 cells transduced with a complex of Ad/Δfiber-L2 and SuperFect

SK HEP-1 cells were transduced with Ad/Δfiber-L2 (30000 VP/cell) in the presence of SuperFect (0, 1.5, or 15 μg) for 3 hr. After 2 days culture period, luciferase production in the cells was determined. The data are expressed as means ±S.D. (n=6).

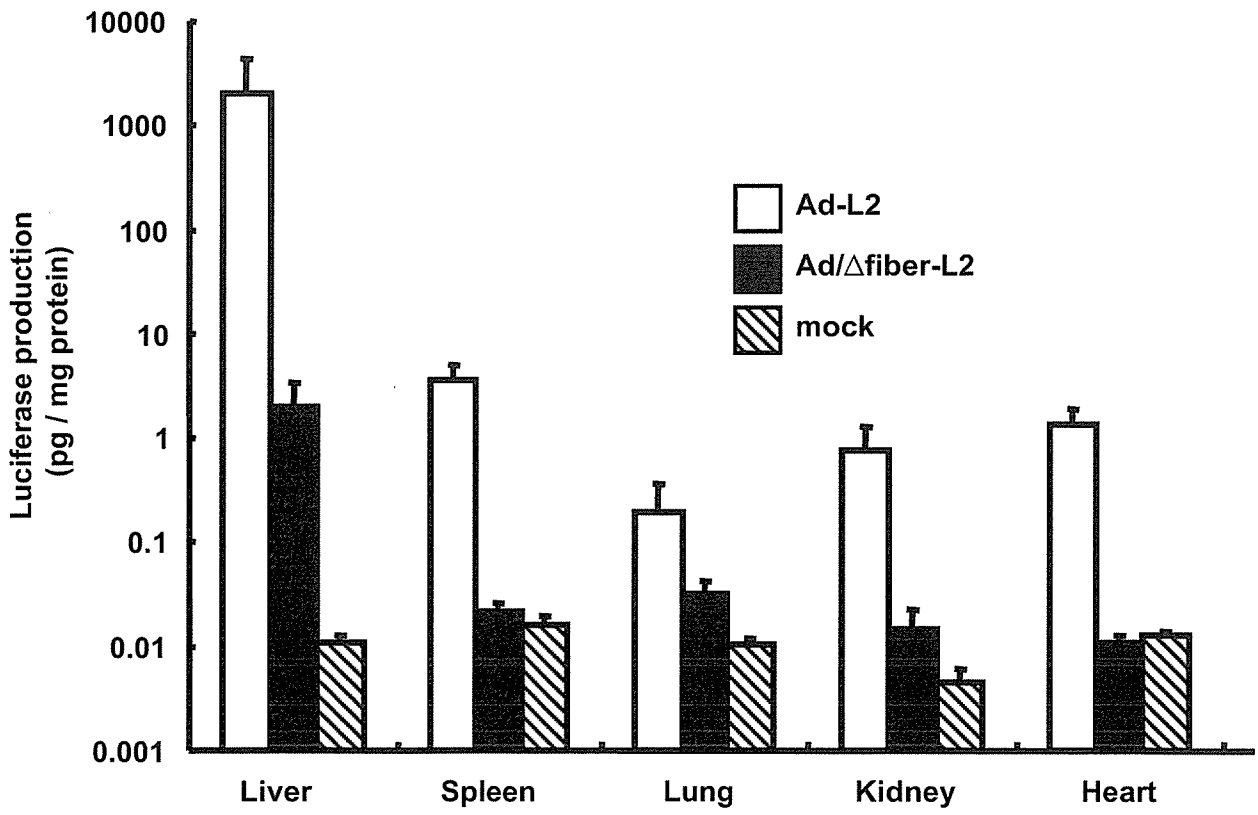

Fig. 57 Luciferase production in mice after the systemic administration of Ad-L2 or Ad/Δfiber-L2.

Ad-L2 or Ad/Δfiber-L2 were intravenously (1.0×10^{10} VP) injected into the mice. Two days later, the liver, spleen lung, kidney, and heart were harvested, and luciferase production was determined. All data represent the means ± S.D. of 5 mice.

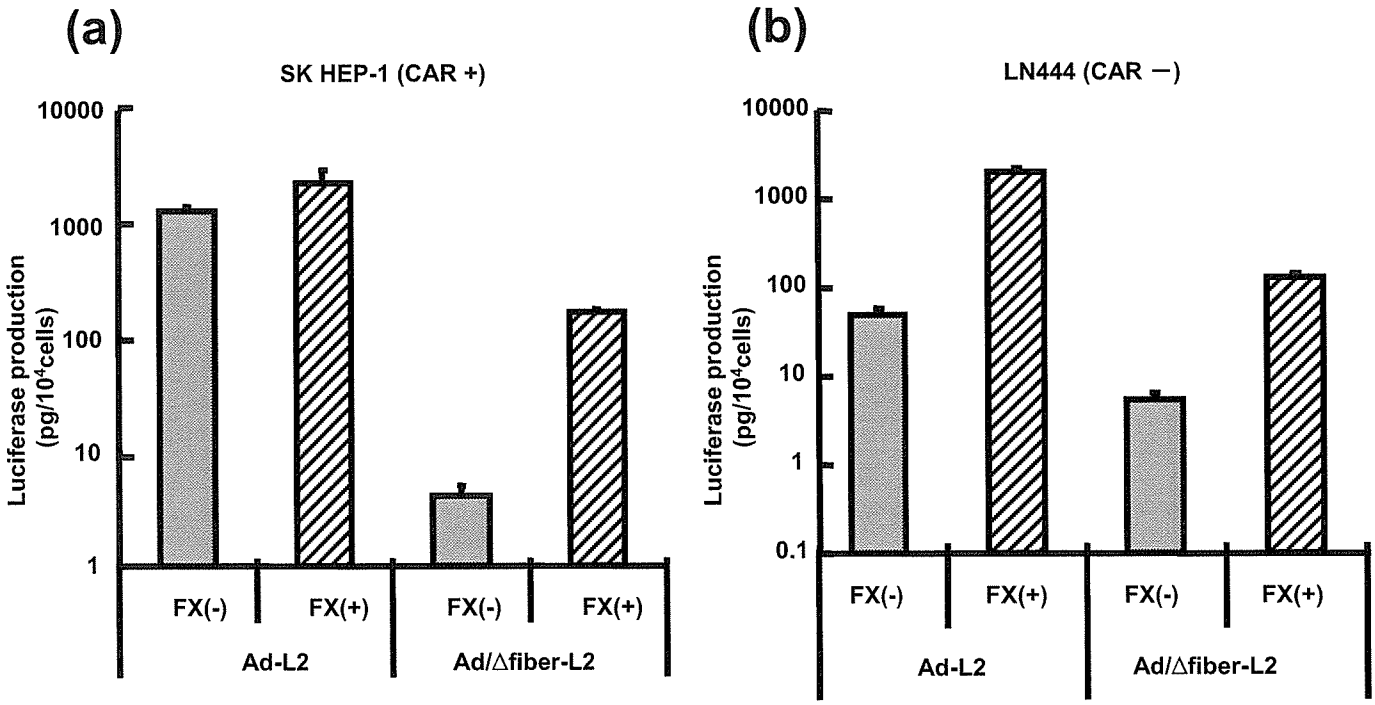

Fig. 58 Effect of the coagulation factor on transduction efficiency of fiber-less Ad vector
SK HEP-1 (1×10^4) cells were transduced with Ad-L2 or Ad/Δfiber-L2 (3000 VP/cell) for 2 hr in the presence or absence of the coagulation factor (FX; 0.4 μg). After 2 days culture period, luciferase production in the cells was determined. The data are expressed as means ±S.D. (n=5).

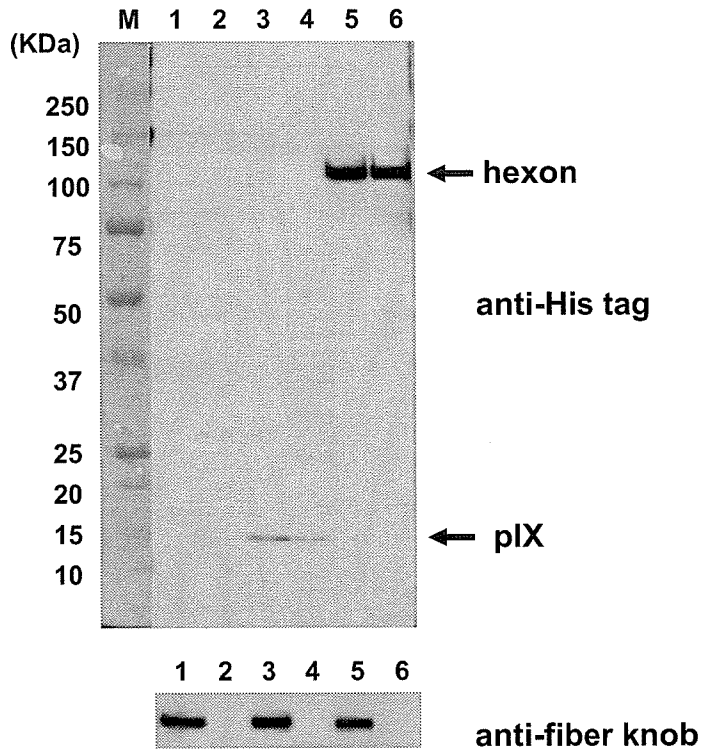

Fig. 59 Western blotting of several types of capsid-modified Ad vectors
The total protein (500 ng) of each vector in 1 × sample buffer containing 4% β-mercaptoethanol was separated on a 4-20% SDS-PAGE gel, and the His tag sequence or the fiber protein was analyzed by Western blotting using anti-His tag antibody or a rabbit fiber knob polyclonal antibody, respectively.
Lane 1, Ad-L2; Lane 2, Ad/Δfiber-L2; Lane 3, Ad-His(pIX)-L2; Lane 4, Ad/Δfiber-His(pIX)-L2; Lane 5, Ad-His(hexon)-L2; Lane 6, Ad/Δfiber-His(hexon)-L2.

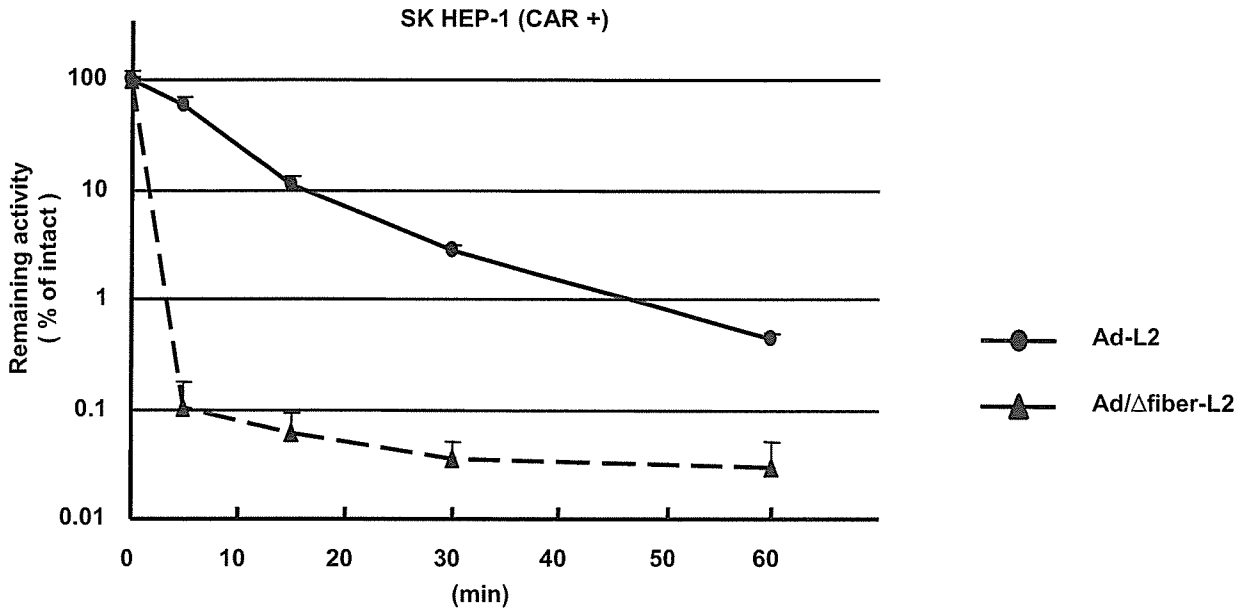

Fig. 60 Physical stability of fiber-less Ad vector

Ad-L2 and Ad/Δfiber-L2, which were suspended with PBS, were incubated at 45 ℃ for different time intervals. Then Ad vectors were added to SK HEP-1 cells (Ad-L2; 3000 VP/cells, Ad/Δfiber-L2; 30000 VP/cells). After 2 days culture period, luciferase production in the cells was determined. The data are expressed as means ±S.D. (n=4).

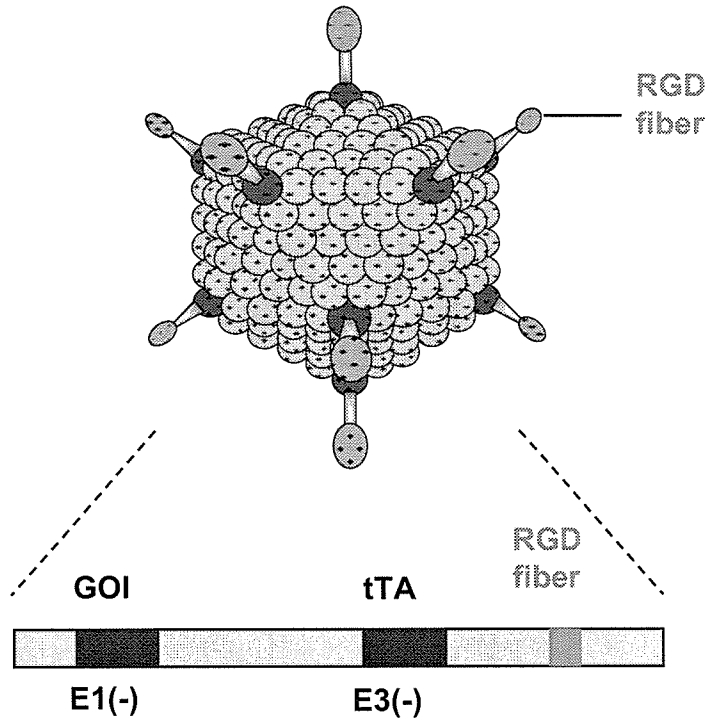

Fig.61 Capsid-modified single adenovirus vectors containing tet-off system

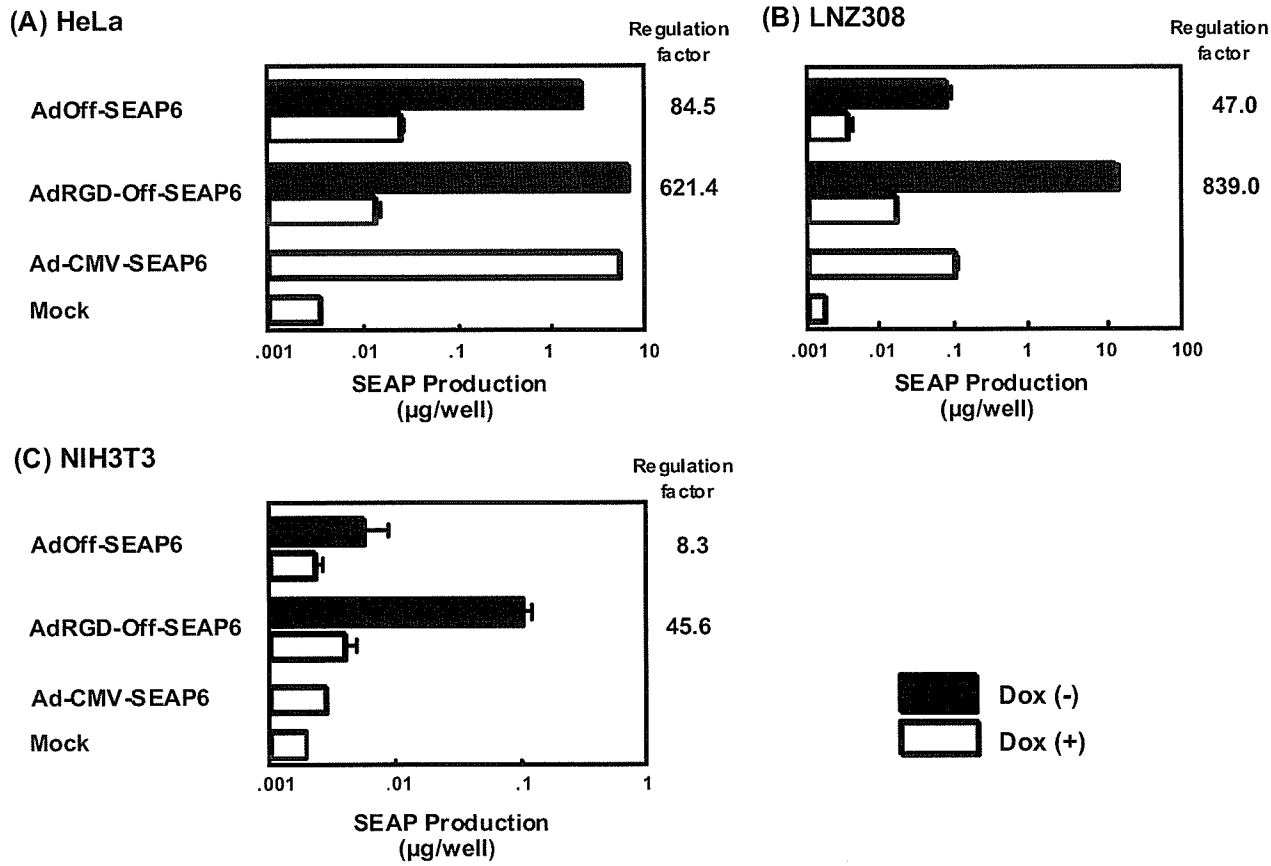

Fig.62 Regulated SEAP production in CAR-positive and -negative cells transduced by capsid-modified single adenovirus vectors containing tet-off system.

HeLa (A), LNZ308 (B), and NIH3T3 (C) cells were transduced with each Ad vector (300 VP/cell). The cells were cultured without (closed columns) and with (slashed columns) 10 ng/ml of doxycycline for 48 h. SEAP production in the medium was determined. Each data represents the mean S.D. of four experiments.

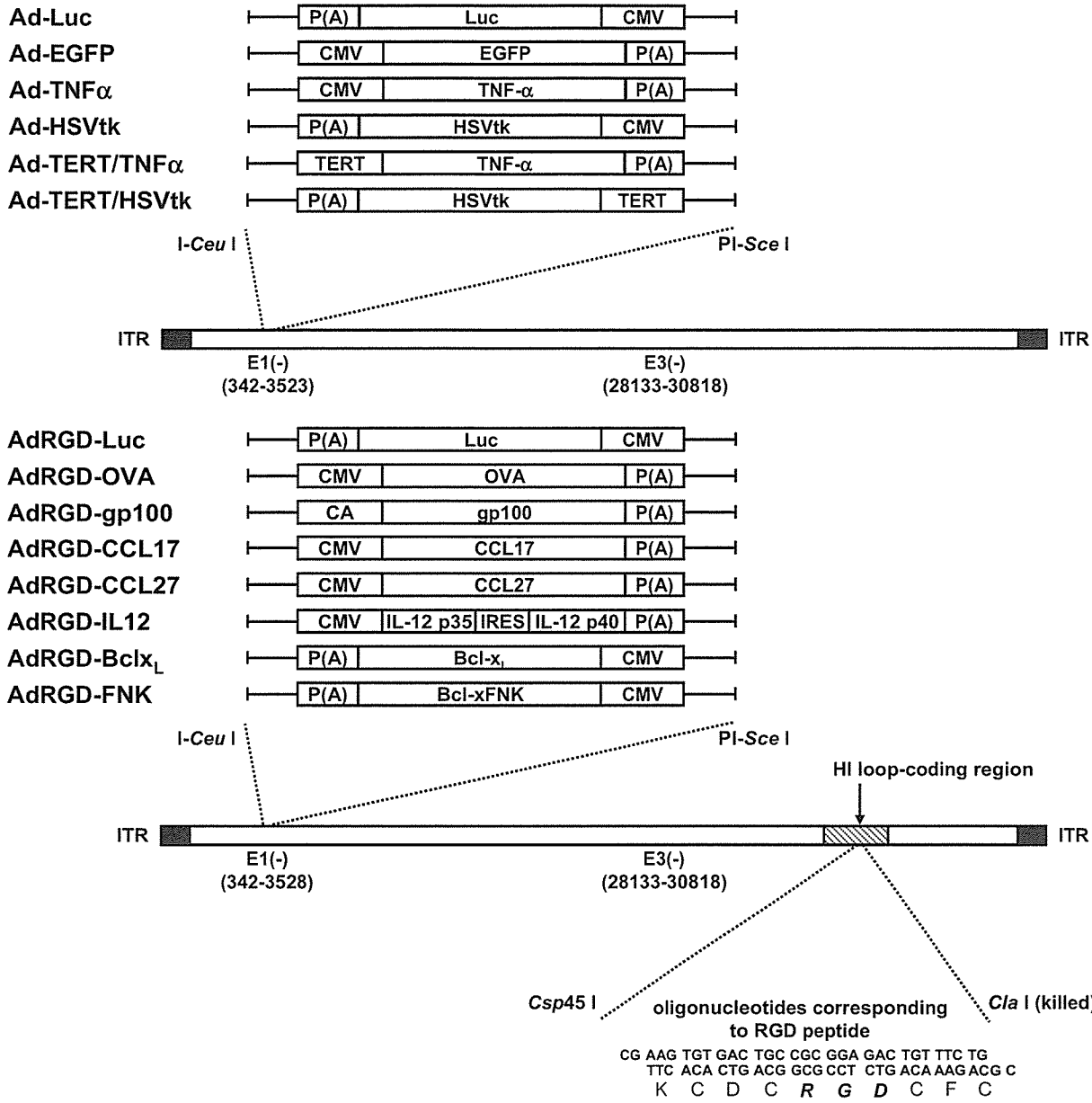

Fig. 63 Schematic representation of Ad vectors used in this study.

Table 9 Primer sequences and reaction parameter used for PCR amplification.

Gene	Primer sequence (5' to 3')	Denaturation	Annealing	Extension	Cycle No.	Product size
Perforin	(F) TTTCGCCTGGTACAAAAACC (R) CAGTCCTGGTTGGTGACCTT	for 30 s at 95°C	for 30 s at 60°C	for 30 s at 72°C	30	680 bp
Granzyme B	(F) CTCGACCCTACATGGCCTTA (R) GAAAGGAAGCACGTTTGGTC	for 30 s at 95°C	for 30 s at 62°C	for 30 s at 72°C	30	507 bp
IFN-γ	(F) GCTTTGCAGCTCTTCCTCAT (R) TGAGCTCATTGAATGCTTGG	for 60 s at 96°C	for 60 s at 50°C	for 60 s at 68°C	30	379 bp
ICAM	(F) CTGGCTGTCACAGAACAGGA (R) AAAGTAGGTGGGGAGGTGCT	for 60 s at 94°C	for 60 s at 54°C	for 60 s at 68°C	30	559 bp
VCAM	(F) CCCAAGGATCCAGAGATTCA (R) TAAGGTGAGGGTGGCATTTC	for 60 s at 94°C	for 60 s at 54°C	for 60 s at 68°C	30	489 bp
β-actin	(F) TGTGATGGTGGGAATGGGTCAG (R) TTTGATGTCACGCACGATTTCC	for 30 s at 95°C	for 30 s at 60°C	for 30 s at 72°C	30	514 bp

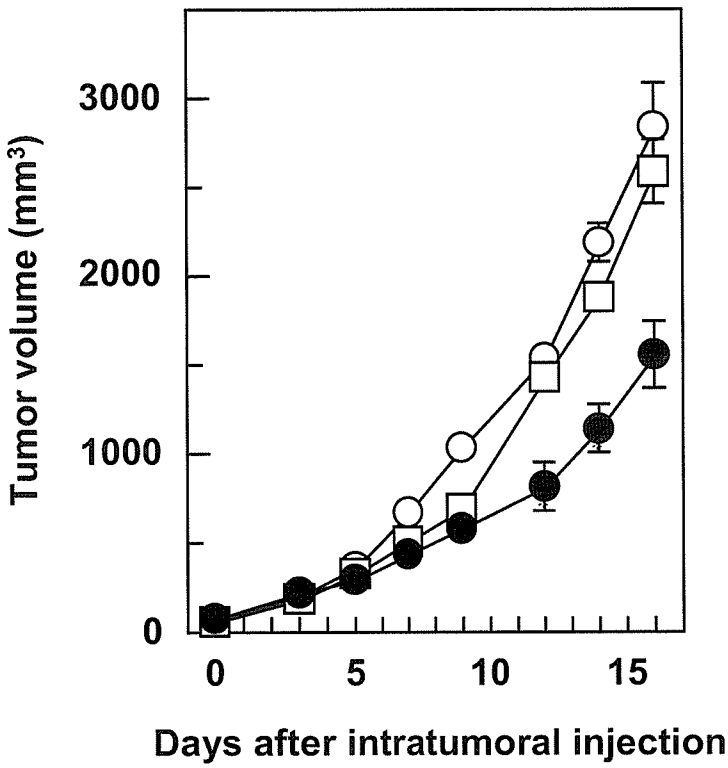

Fig. 64 Anti-B16BL6 tumor efficacy of intratumorally injected AdRGD-CCL17. B16BL6 cells were intradermally inoculated into the right flank of C57BL/6 mice at 4×10^5 cells/mouse. The tumors (5-7 mm in diameter) were injected with AdRGD-CCL17 (●) or AdRGD-Luc (□) at 3×10^8 PFU. Likewise, PBS (○) was injected into the tumors. The tumor volume was calculated after measuring the major and minor axes of the tumor at indicated points. Each point represents the mean ± SE from 6-10 mice.

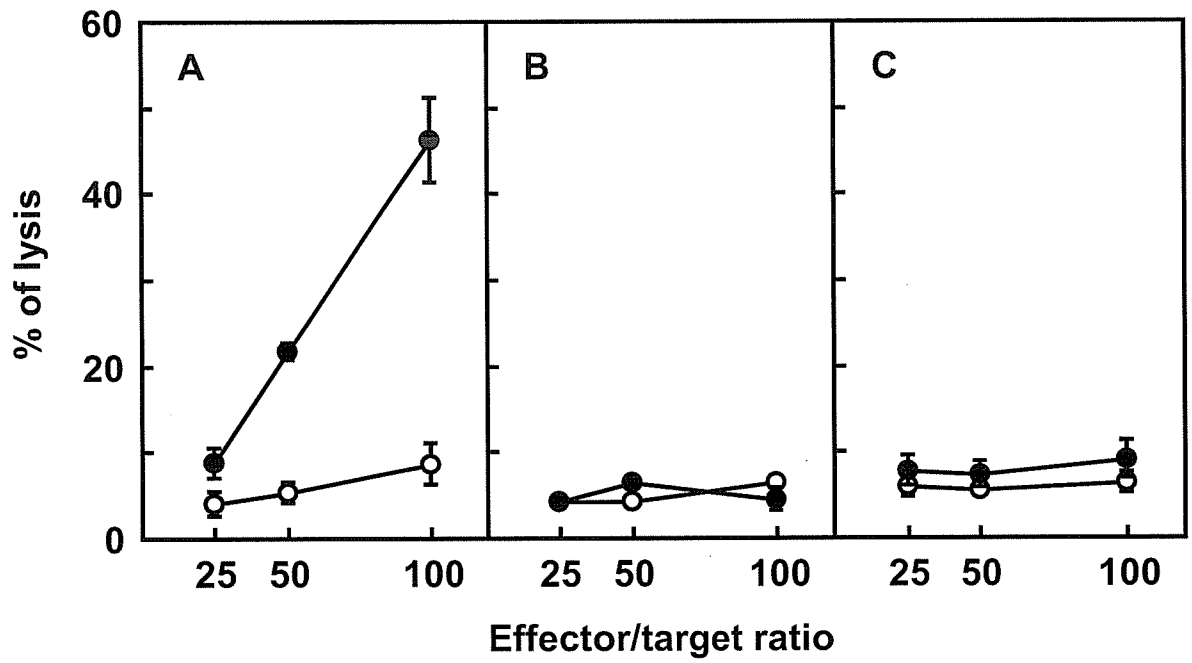

Fig. 65 Enhanced tumor-specific CTL activity in B16BL6 tumor-bearing mice by gp100/DC-immunization. B16BL6 cells were intradermally inoculated into the right flank of C57BL/6 mice at 4×10^5 cells/mouse. One day later, the mice were intradermally injected with 10^6 gp100/DCs (●) or PBS (○) in the left flank. At 1 week after immunization, non-adherent splenocytes were prepared from these mice, and then were re-stimulated *in vitro* for 5 days with IFN-γ-stimulated and mitomycin C-inactivated B16BL6 cells. A cytolytic assay using the re-stimulated splenocytes was performed against IFN-γ-stimulated B16BL6 (A), IFN-γ-stimulated EL4 (B), and YAC-1 (C) cells. The data represent the mean ± SE of three independent cultures from three individual mice.

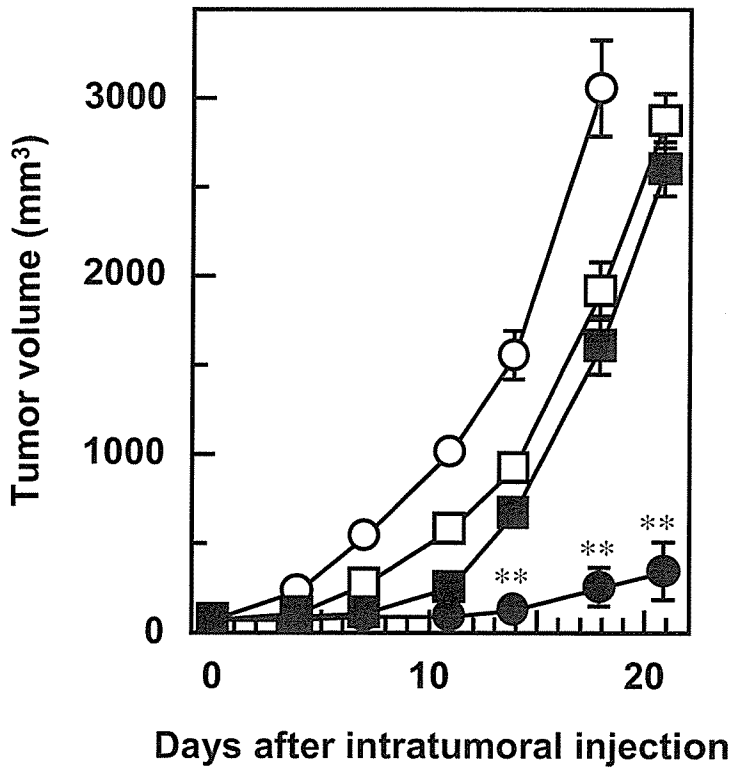

Fig. 66 Anti-B16BL6 tumor efficacy of intratumorally injected AdRGD-CCL17 in combination with gp100/DC-immunization. B16BL6 cells were intradermally inoculated into the right flank of C57BL/6 mice at 4×10^5 cells/mouse. The next day post-tumor inoculation, the mice were intradermally immunized with 10^6 gp100/DCs (●,■,□) or PBS (○) in the left flank. Then, the tumors (5-7 mm in diameter) were injected with AdRGD-CCL17 (●) or AdRGD-Luc (■) at 3×10^8 PFU. Likewise, PBS was administered into control tumors in mice pretreated with gp100/DCs (□) or PBS (○). Tumor volume was calculated after measuring the major and minor axes of the tumor at indicated points. Each point represents the mean ± SE of 7-15 mice. Statistical analysis was carried out by Mann-Whitney *U*-test: *; $p < 0.01$, **; $p < 0.001$ versus AdRGD-Luc-injected group (■).

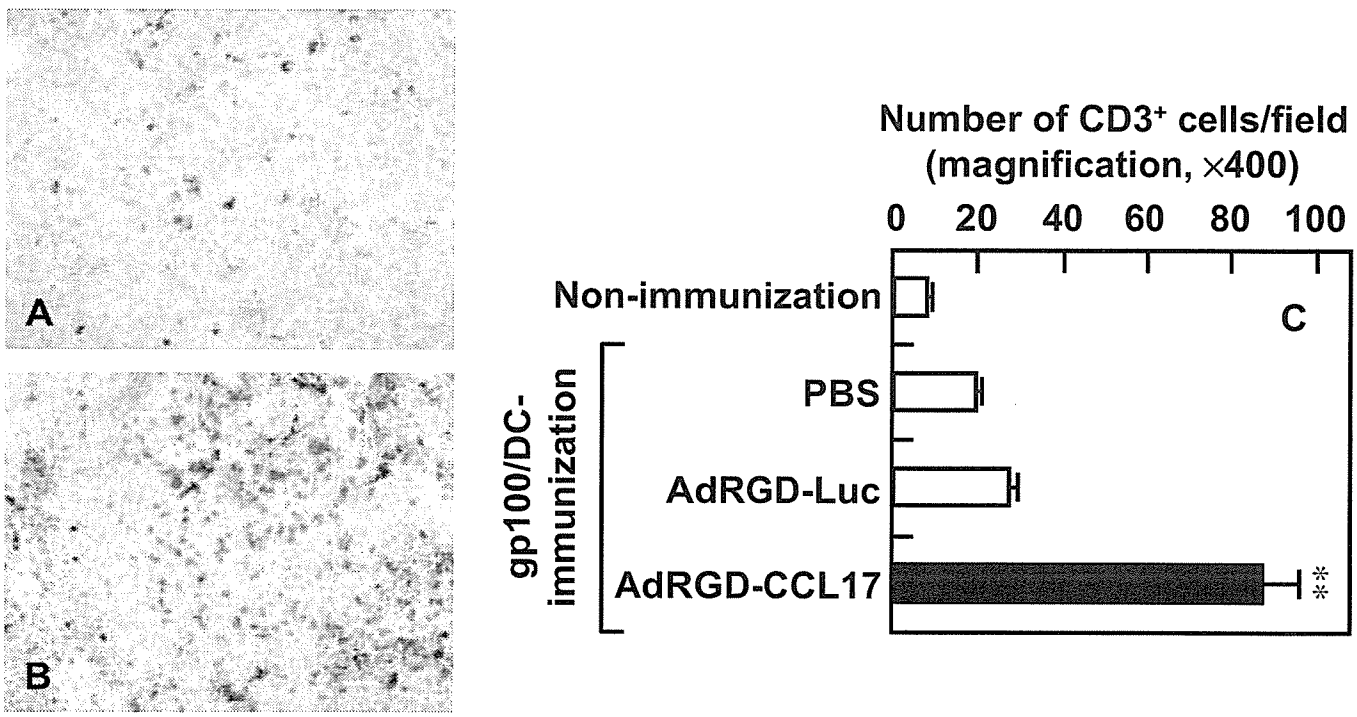

Fig. 67 Infiltration of T cells into B16BL6 tumors of mice treated with the combination of gp100/DC-immunization and intratumoral injection of AdRGD-CCL17. B16BL6 cells were intradermally inoculated into the right flank of C57BL/6 mice at 4×10^5 cells/mouse. The next day, the mice were intradermally injected with 10^6 gp100/DCs in the left flank. Then, the tumors (5-7 mm in diameter) were injected with AdRGD-Luc (A) or AdRGD-CCL17 (B) at 3×10^8 PFU. Likewise, PBS was administered into control tumors. On day 2 after intratumoral injection, immunohistochemical staining against CD3 for determining T cells was performed with frozen tumor sections. A and B; original magnifications are ×200. C; the number of CD3-positive cells in the intratumoral section was assessed by counting six fields per specimen under ×400-magnification. The data represent the mean ± SE of results from three tumors. Statistical analysis was carried out by Welch's *t*-test: **; $p < 0.001$ versus AdRGD-Luc-injected group.

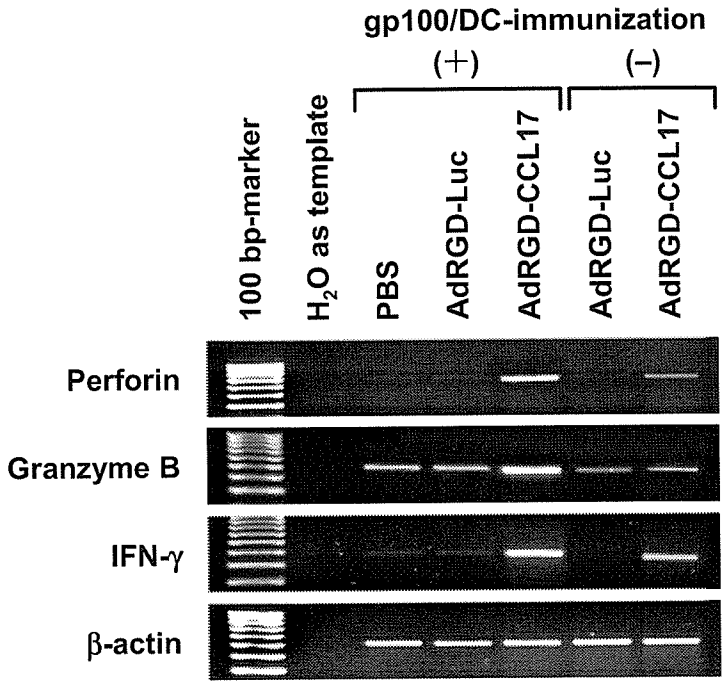

Fig. 68 Activation state of infiltrating immune cells in B16BL6 tumors injected intratumorally with AdRGD-CCL17 in combination with or without gp100/DC-immunization. B16BL6 cells were intradermally inoculated into the right flank of C57BL/6 mice at 4×10^5 cells/mouse. One day later, the mice were intradermally injected with or without 10^6 gp100/DCs in the left flank. The tumor (5-7 mm in diameter) was injected with AdRGD-CCL17 or AdRGD-Luc at 3×10^8 PFU. Likewise, PBS was administered into control tumors. Two days later, total RNA was isolated from the tumors collected from these mice, and then RT-PCR, specific for perforin, granzyme B, and IFN-γ transcripts, was performed. The PCR products were electrophoresed through a 3% agarose gel, stained with ethidium bromide, and visualized under ultraviolet light.

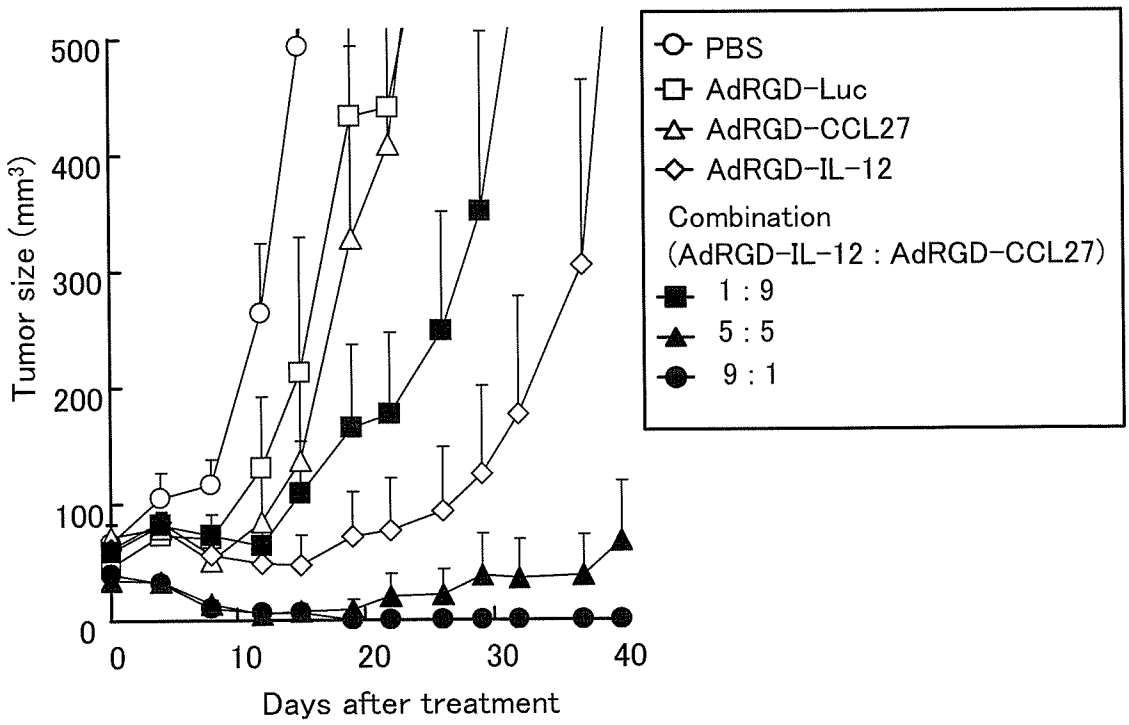

Fig. 69 Combination of AdRGD-IL-12 and AdRGD-CCL27 induced synergistic anti-tumor activity. B6C3F1 mice 1×10^6 OV-HM cells were inoculated intradermally into B6C3F1 mice. After the tumor diameter reached 7-8mm, indicated adenovirus vectors in total of 2×10^7 PFU or PBS were injected intratumorally. Tumor size was measured twice a week.

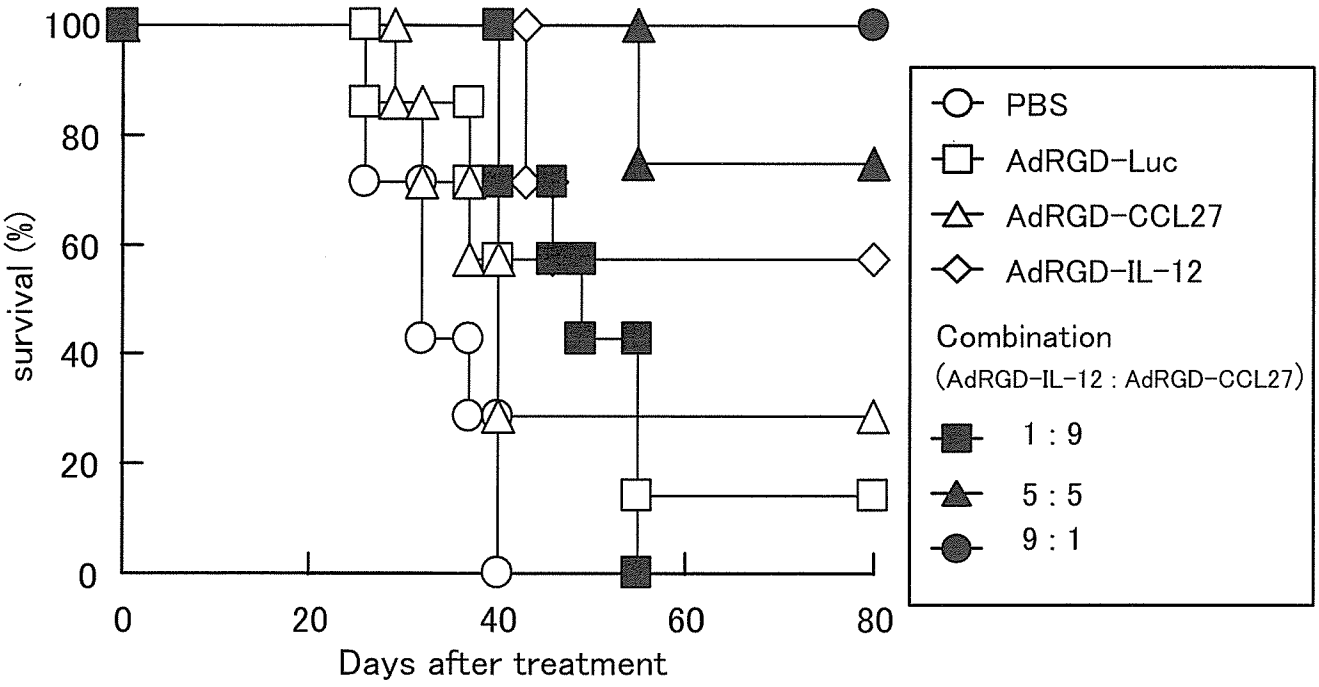

Fig. 70 The survival percent of mice with the treatment of indicated adenovirus vectors

Table 10 Induction of specific long-term immunity against OV-HM cells in tumor rejected mice.

Groups	Challenging cells	Tumor rejected mice/ challenged mice		
		After 3 months		After 6 months
		1st Exp.	2nd Exp.	3rd Exp.
Intact	OV-HM	0/6	0/6	0/6
Combination AdRGD-IL-12 (9) / AdRGD-CCL27 (1)	OV-HM	4/5	5/5	5/5
	B16BL6	0/3	0/5	0/5
Combination AdRGD-IL-12 (5) / AdRGD-CCL27 (5)	OV-HM	4/4		
	B16BL6	0/2		

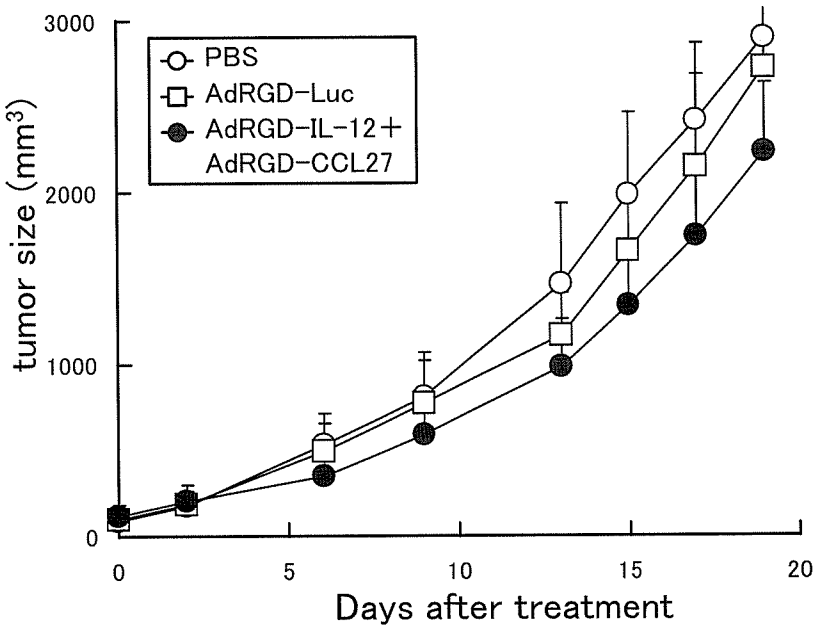

Fig. 71 Anti-tumor effect induced by the combination of AdRGD-IL-12 and AdRGD-CCL27 is T cell-dependent. Balb/c nude mice were inoculated intradermally with OV-HM cells (1×10^6 cells/mouse). After one week, 50 μl of PBS, 2×10^7 PFU of AdRGD-Luc, or AdRGD-IL-12 plus AdRGD-CCL27, in total of 2×10^7 PFU at the ratio of 9:1, were intratumorally injected . Tumor size was measured twice a week.

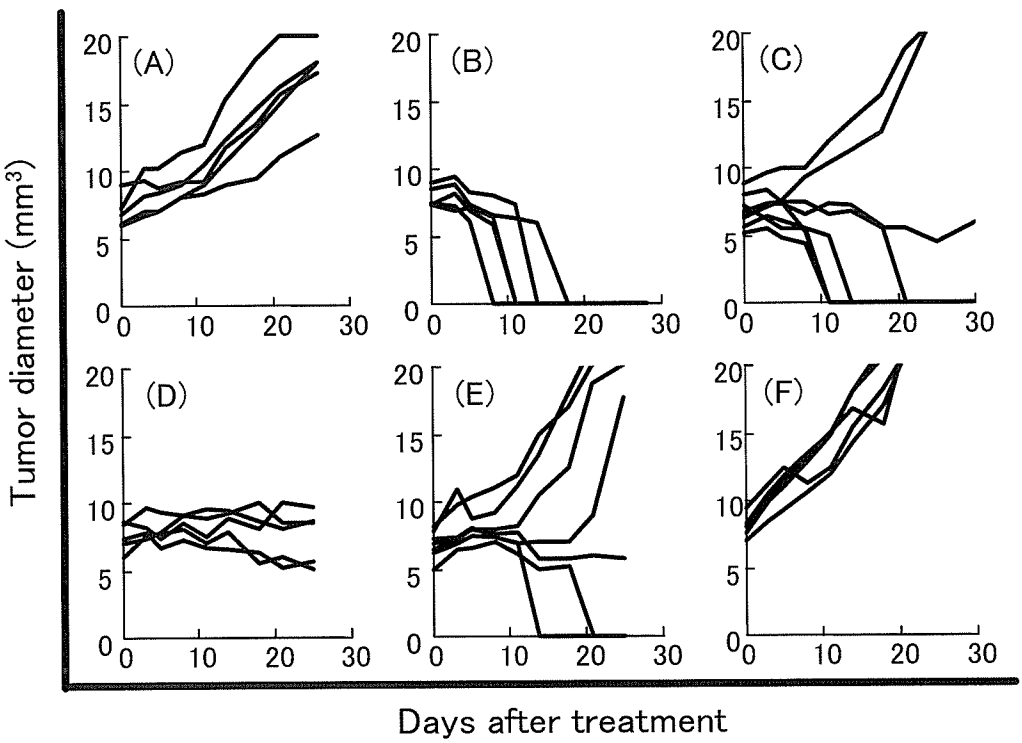

Fig. 72 Both CD4 or CD8 T cells contributed to the anti-tumor activity induced by combination. CD4 positive T, CD8 positive T or NK cell-depleted naive mice were inoculated intradermally with OV-HM cells (1×10^6 cells/mouse). (A) Tumor-bearing mice treated with PBS, (B) intact mice, (C) NK cell-depleted mice, (D) CD4 positive T cell-depleted mice, (E) CD8 positive T cell-depleted mice, (F) CD4 positive T cell and CD8 positive T cell-depleted mice treated with AdRGD-IL-12 and AdRGD-CCL27 at a ratio of 9:1 (in total 2×10^7 PFU/mouse).

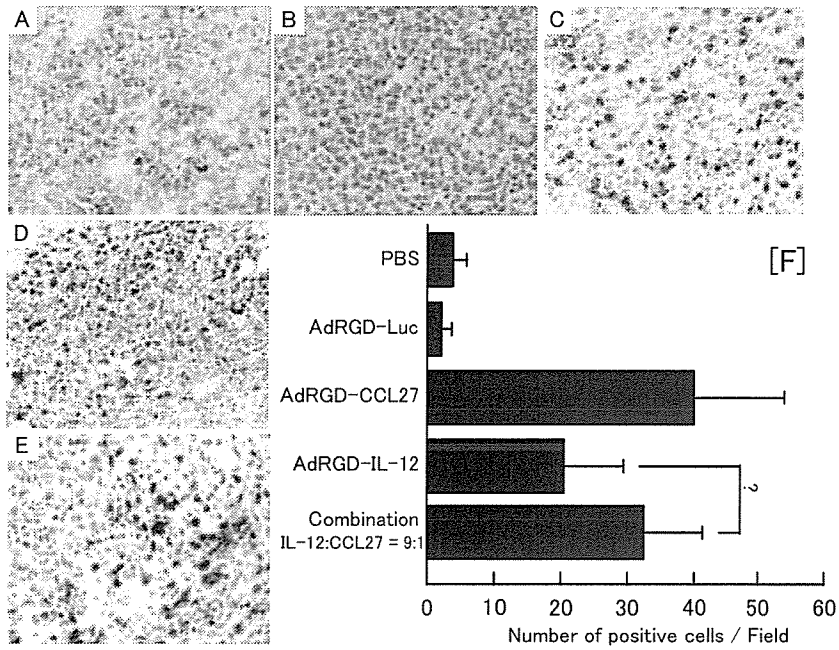

Fig. 73 CD3 positive lymphocyte infiltrate into OV-HM tumor. Immunohistochemical analysis was utilized to determine lymphocytes infiltrated into tumors. When the length of tumor reached about 7-8 mm, intratumoral administrations of indicated adenovirus vectors were carried out. Tumor-bearing mice were sacrificed in six days after the intratumoral administration of (A) PBS, (B) AdRGD-Luc, (C) AdRGD-CCL27, (D) AdRGD-IL-12 or (E) combination (AdRGD-IL-12:AdRGD-CCL27=9:1). The tumor nodules were harvested, embedded in the O.C.T. compound, and stored at -80℃. Frozen thin sections of the nodules were fixed and stained for CD3 positive T cells using the method described above. (F) The number of immunostained cells were counted under light microscope with ×400 magnihication. For countinf positive cell number infiltrated into tumor tissue, six fields were randomly selected. Statistical analysis was carried out by Student's t-test. ✻; < 0.05

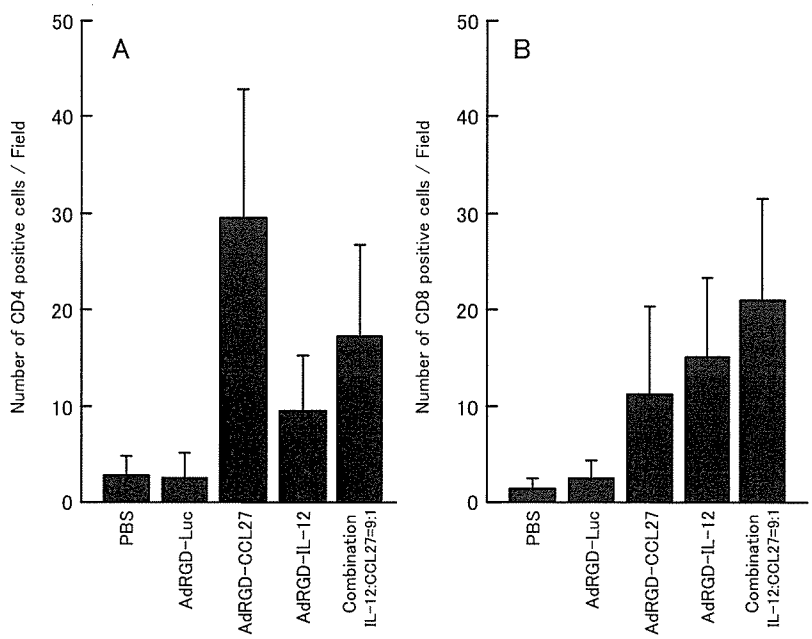

Fig. 74 CD4 or CD8 positive lymphocyte infiltrate into OV-HM tumor. When the length of tumor reached about 7-8 mm, intratumoral administrations of indicated adenovirus vectors were carried out. Tumor-bearing mice were sacrificed in six days after the intratumoral administration of AdRGD-CCL27, AdRGD-IL-12 or combination. The tumor nodules were harvested, embedded in the O.C.T. compound., stored at -80℃. Frozen thin sections of the nodules were fixed and stained for CD4 (A) or CD8 (B)-positive cells using the method described above. The number of immunostained cells were counted under light microscope with ×400 magnification. For counting the positive cell number infiltrated into tumor tissue, six fields were randomly selected.

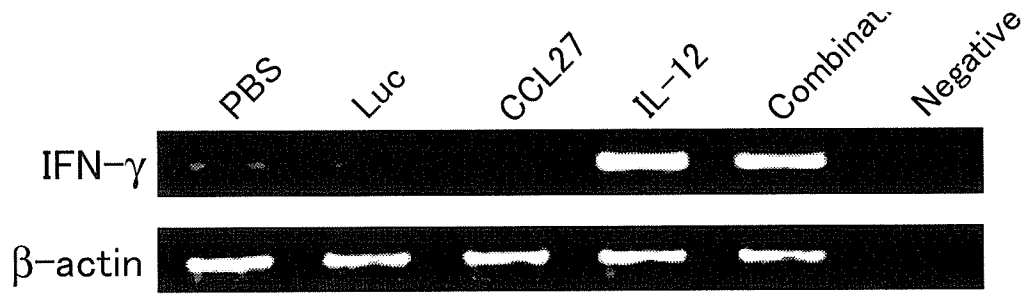

Fig. 75 RT-PCR analysis of murine IFN-γ in indicated adenovirus vectors injected OV-HM tumor nodules. Total RNA was extracted from OV-HM tumor nodules, and then RT-PCR was performed to amplify the mRNA levels of mouse IFN-γ (379bp) and β-actin (514bp). PCR products were visualized by ethidium bromide staining after electrophoresis on an agarose gel. Negative was performed PCR using water as template.

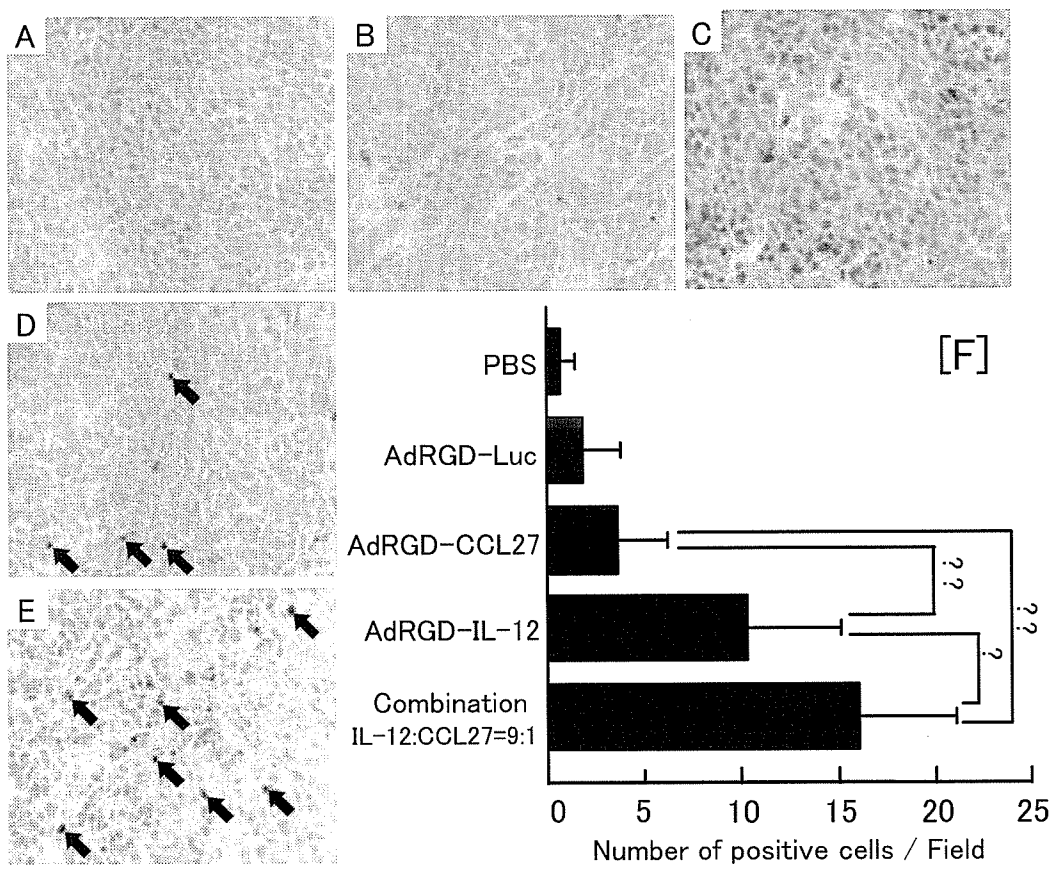

Fig. 76 Perforin positive cells infiltrate into OV-HM tumor. When the length of tumor reached about 7-8 mm, intratumoral administrations of indicated adenovirus vectors were carried out. Tumor-bearing mice were sacrificed in six days after the intratumoral administrations of (A) PBS, (B) AdRGD-Luc, (C) AdRGD-CCL27, (D) AdRGD-IL-12 and (E) combination (AdRGD-IL-12:AdRGD-CCL27=9:1). The tumor nodules were harvested, embedded in the O.C.T. compound, and stored at -80℃. Frozen thin sections of the nodules were fixed and stained for perforin-positive cells using the method described above. The number of immunostained cells were counted under light microscope with ×400 magnification. For counting the positive cell number infiltrated into tumor tissue, 6 fields were randomly selected. (F) Quantitation of perforin-positive cells in treated tumors. Statistical analysis was carried out by Student's t-test. ✻; < 0.05, ✻✻; < 0.01

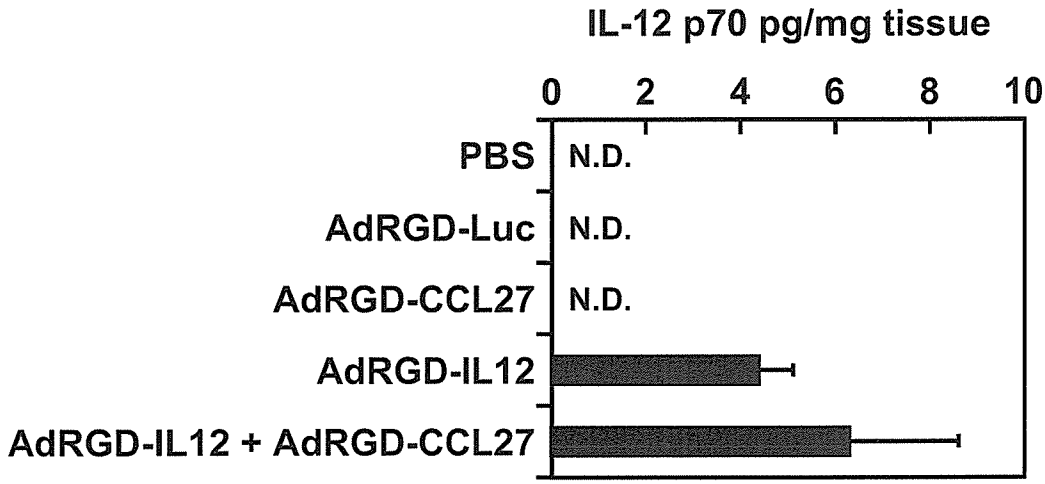

Fig. 77 IL-12 production levels in Meth-A tumors injected with AdRGD-IL12 alone or combined with AdRGD-CCL27. BALB/c mice were intradermally inoculated with 2×10^6 Meth-A cells into the flank. The tumors (9-10 mm in diameter) were injected with AdRGD-Luc alone, AdRGD-CCL27 alone, AdRGD-IL12 alone, or AdRGD-IL12 plus AdRGD-CCL27 in a ratio of 9:1 at the same dose totaling 2×10^7 PFU. PBS was injected into the tumors as a control. Two days later, the tumors were harvested, and then IL-12p70 levels in their homogenates were measured by ELISA. The data represent the mean ± SD of results from three tumors. N.D.: not detectable.

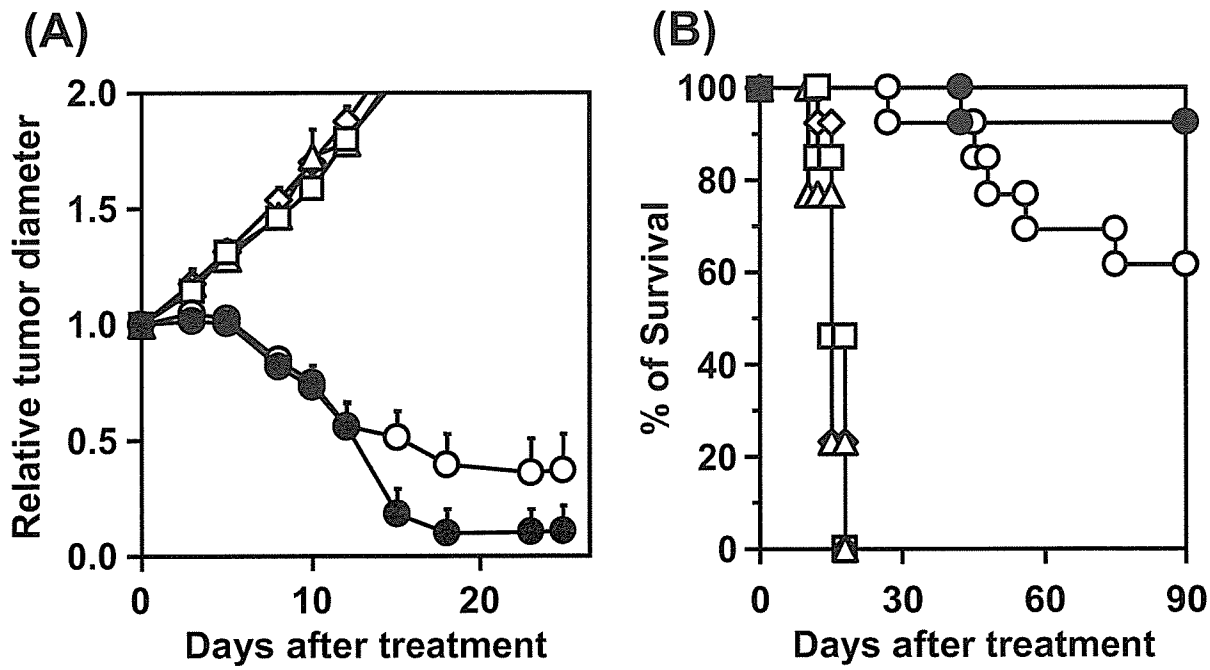

Fig. 78 Antitumor efficacy of intratumorally injected AdRGD-IL-12 plus AdRGD-CCL27 in Meth-A tumor model. BALB/c mice were intradermally inoculated with 2×10^6 Meth-A cells into the flank. The tumors (7-9 mm in diameter) were injected with either AdRGD-Luc alone (△), AdRGD-IL-12 alone (○), AdRGD-CCL27 alone (□), or the combination of AdRGD-IL-12 and AdRGD-CCL27 in a ratio of 9:1 (●) at the same dose totaling 2×10^7 PFU. PBS (◇) was injected into the tumors as a control. (A): The sizes of growing tumors were measured twice a week using microcalipers. Data are expressed as the ratio to the initial tumor diameter. Each point represents the mean ± SE of results from 7 or 8 mice. (B): Data represent the number of mice for which tumors were smaller than 20 mm, expressed as a percentage of the total mice tested in each group.

Table 11 Induction of long-term specific immunity in mice which could achieve complete regression of the primary Meth-A tumor by intratumoral injection with either AdRGD-IL12 alone or the combination of AdRGD-IL12 and AdRGD-CCL27.

Groups	Rechallenging cells[a)]	Tumor-rejected mice/ tested mice
Intact mice	Meth-A	0/10
	CT26	0/5
Meth-A-regressed mice by the injection with AdRGD-IL12	Meth-A	9/9
	CT26	0/6
Meth-A-regressed mice by the injection with AdRGD-IL12 + AdRGD-CCL27	Meth-A	12/12
	CT26	0/5

[a)] Meth-A or CT26 cells were inoculated at 10^6 or 10^5 cells/mouse, respectively.

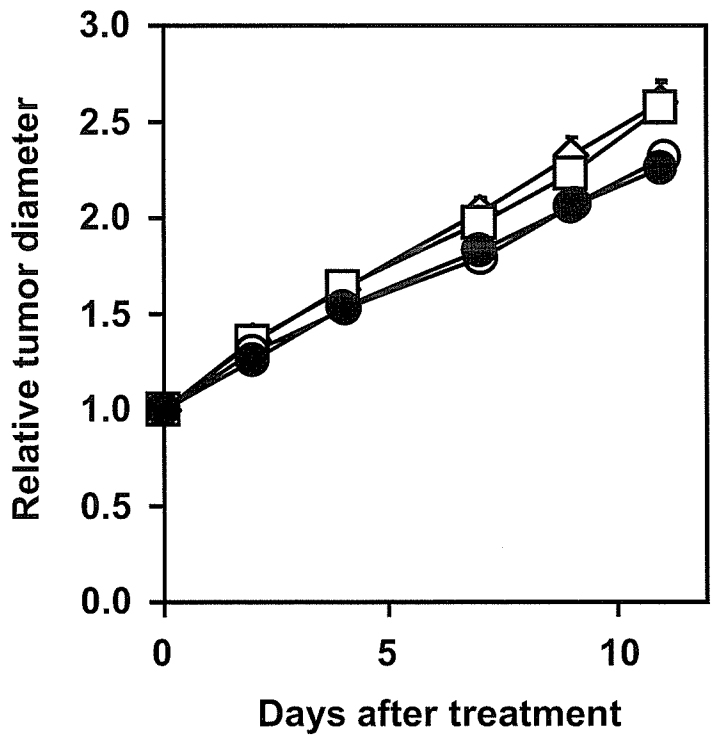

Fig. 79 Growth of Meth-A tumors injected with the AdRGD-IL-12 and AdRGD-CCL27 combination in athymic BALB/c nude mice. BALB/c nude mice were intradermally inoculated with 2×10^6 Meth-A cells into the flanks. The tumors (7-9 mm in diameter) were injected with AdRGD-Luc alone (□), AdRGD-IL12 alone (○), or AdRGD-IL12 plus AdRGD-CCL27 in a ratio of 9:1 (●) at the same dose totaling 2×10^7 PFU. PBS (△) was injected into the tumors as a control. The sizes of growing tumors were measured using microcalipers. Data are expressed as the ratio to the initial tumor diameter. Each point represents the mean ± SE of results from at least six mice.

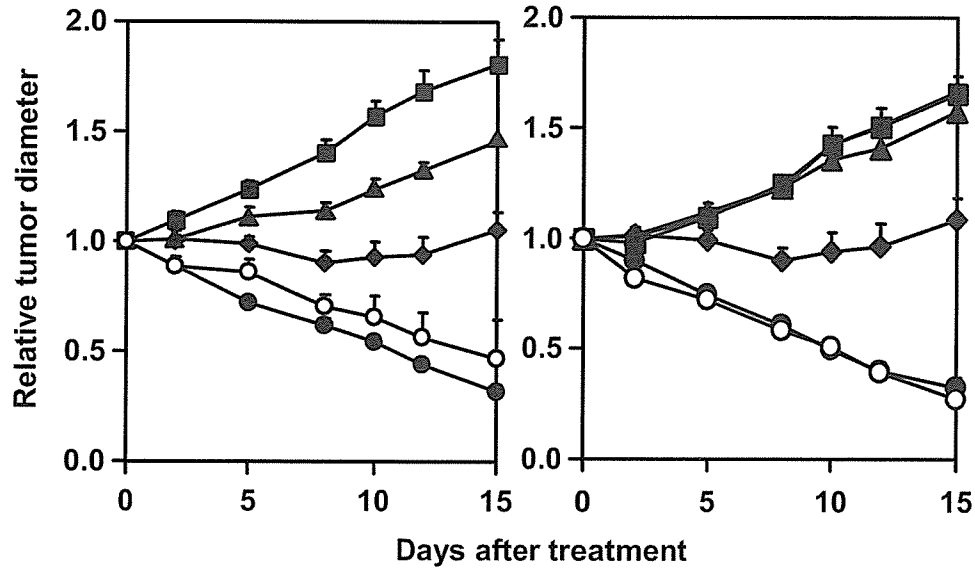

Fig. 80 Determination of immune subsets responsible for the antitumor efficacy induced by the IL-12/CCL27 combination. On day -7, BALB/c mice were intradermally inoculated with 2×10^6 Meth-A cells into the flanks. For depletion of $CD4^+$ T cells (●), $CD8^+$ T cells (▲), or NK cells (◆) in the mice, GK1.5 ascites (anti-CD4), 53-6.72 ascites (anti-CD8), or anti-asialoGM1 antisera were intraperitoneally injected on days -3, -2, -1, 0, 5, 10, and 15. Likewise, for depletion of both $CD4^+$ and $CD8^+$ T cells (■), mice were injected with GK1.5 ascites and 53-6.72 ascites. Normal rat serum (○) was injected into the mice as a control. On day 0, Meth-A tumors received the AdRGD-IL12/AdRGD-CCL27 combination intratumoral injection in a ratio of 9:1 totaling 2×10^7 PFU. Tumor growth was monitored twice a week. Data are expressed as the ratio to the initial tumor diameter. Each point represents the mean ± SE of results from 5-7 mice.

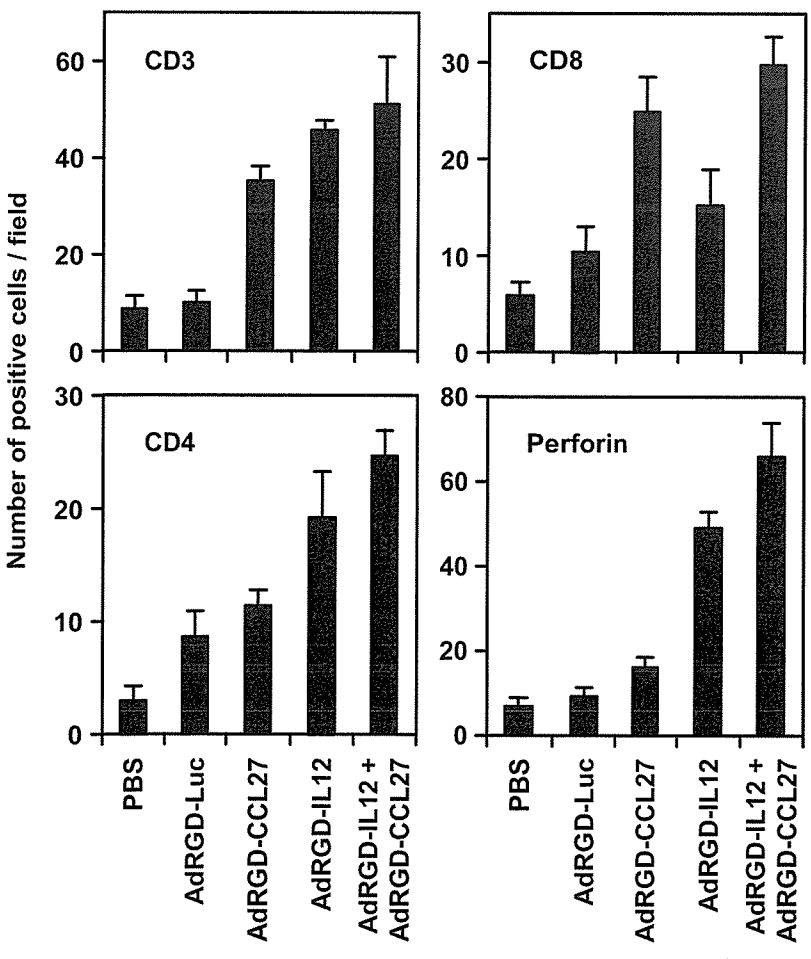

Fig. 81 Quantification of tumor-infiltrating T cell subsets and perforin-positive cells in Meth-A tumors injected with the IL-12/CCL27 combination. Meth-A cells were intradermally inoculated into the flanks of BALB/c mice at 2×10^6 cells/mouse. The tumors (7-9 mm in diameter) were injected with AdRGD-Luc alone, AdRGD-CCL27 alone, AdRGD-IL12 alone, or the AdRGD-IL12 and AdRGD-CCL27 combination in a ratio of 9:1 at the same dose totaling 2×10^7 PFU. PBS was injected into the tumors as a control. On day 6 after the intratumoral injections, immunohistochemical staining against CD3, CD4, and CD8 was performed using frozen tumor sections. These immunohistochemical sections were used to assess the numbers of $CD3^+$, $CD4^+$, $CD8^+$, and $perforin^+$ cells infiltrating into tumor parenchyma by counting six fields per specimen under ×400-magnification. The data represent the mean ± SD of results from three tumors.

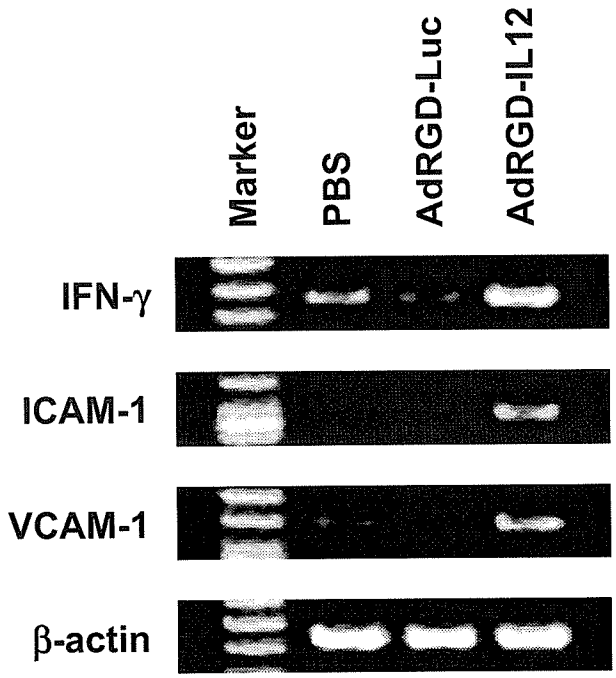

Fig. 82 Increases in expression levels of IFN-γ, ICAM-1, and VCAM-1 in Meth-A tumors injected with AdRGD-IL12. Meth-A cells were intradermally inoculated into the flanks of BALB/c mice at 2×10^6 cells/mouse. The tumors (7-9 mm in diameter) were injected with AdRGD-Luc or AdRGD-IL12 at 2×10^7 PFU. PBS was injected into the tumors as a control. On day 6 after the intratumoral injections, total RNA was isolated from the Meth-A tumors collected from treated mice, and then RT-PCR, specific for IFN-γ, ICAM-1, VCAM-1, and β-actin transcripts, was performed using each primer set descrived in Table 1. The PCR products were electrophoresed through a 2% agarose gel, stained with ethidium bromide, and visualized under ultraviolet light.

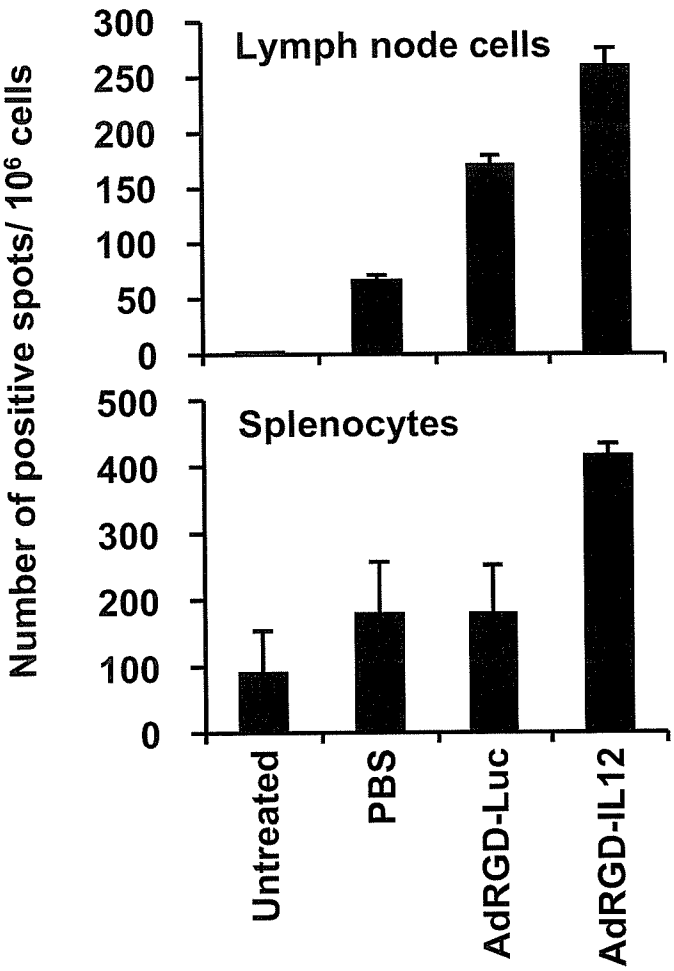

Fig. 83 The frequency of IFN-γ producing cells in draining lymph node cells and splenocytes from Meth-A-bearing mice injected with AdRGD-IL12. BALB/c mice were intradermally inoculated with 2×10^6 Meth-A cells into the flanks. The tumors (7-9 mm in diameter) were injected with AdRGD-Luc or AdRGD-IL12 at 2×10^7 PFU. PBS was injected into the tumors as a control. On day 6 after the intratumoral injections, the draining lymph node cells and splenocytes were prepared from these mice, and then were restimulated *in vitro* with mitomycine C-inactivated Meth-A cells for 24 h. IFN-γ producing cells were evaluated using mouse IFN-γ ELISPOT assay. The data represent the mean ± SE of the results from three mice.

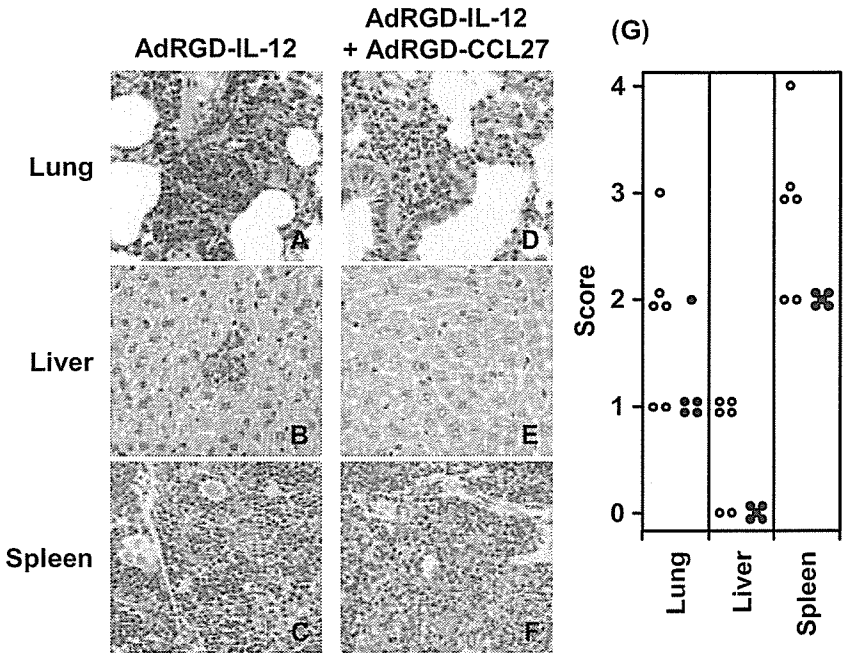

Fig. 84 Histopathological examination of lung, liver, and spleen in Meth-A tumor-bearing mice treated with the AdRGD-IL12/AdRGD-CCL27 combination intratumoral injection. BALB/c mice were intradermally inoculated with 2×10^6 Meth-A cells into the flanks. The tumors (7-9 mm in diameter) were injected with AdRGD-IL12 alone or the AdRGD-IL12 and AdRGD-CCL27 combination in a ratio of 9:1 at the same dose totaling 2×10^7 PFU. Three months later, lung (A and D), liver (B and E), and spleen (C and F) were harvested from mice in which the primary tumors were judged to have completely regressed, and then HE staining was performed using paraffin-embedded tissue sections. Original magnifications are ×300. (G): Histopathological changes (lymphocyte infiltration in lung and extramedullary hematopoiesis in liver and spleen) were scored as: 0, no; 1, rare; 2, mild; 3, moderate; 4, severe. (○); AdRGD-IL12 alone, (●); AdRGD-IL12 plus AdRGD-CCL27.

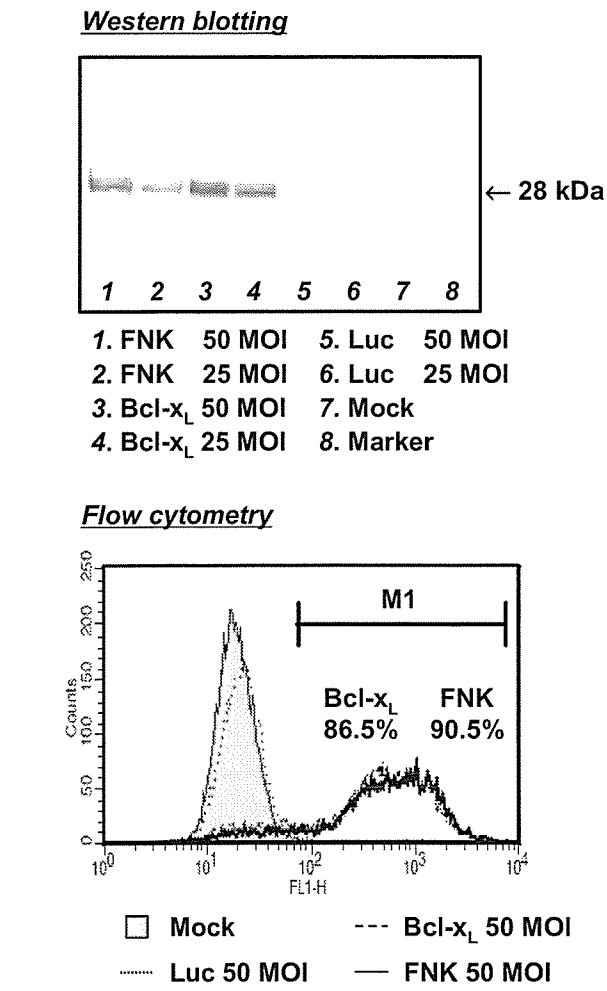

Fig. 85 Gene expression analysis in A549 cells transfected with AdRGD-Bclx$_L$ or AdRGD-FNK. Human A549 cells were transfected with AdRGD-Bclx$_L$, AdRGD-FNK, or AdRGD-Luc at 50 MOI. After 48 h-culutivation, the expression of Bcl-x$_L$ or Bcl-xFNK proteins was assessed by both western blotting and flow cytometry analysis with an intracellular staining method. The % values in the lower panel express the percentage of M1-gated cells.

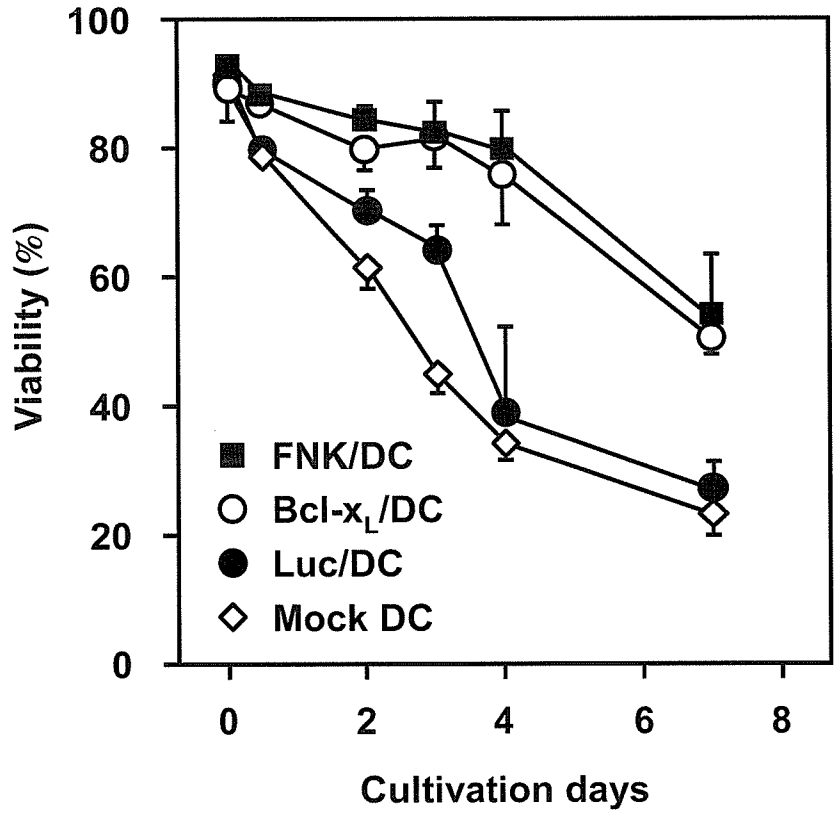

Fig. 86 *In vitro* viability of DCs transfected with AdRGD-Bclx$_L$ or AdRGD-FNK. FNK/DCs, Bcl-x$_L$/DCs, and Luc/DCs were prepared using corresponding vectors at 25 MOI, and then these transduced cells and mock DCs were cultured without cytokines and growth factors. The viability of DCs was assessed by propidium iodide staining at indicated cultivation days. Each point represents the means ± SE of triplicate cultures.

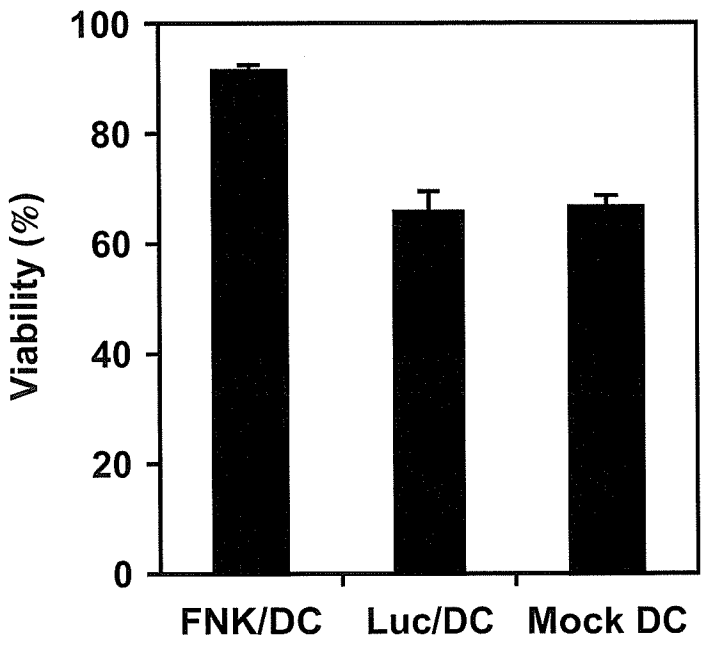

Fig. 87 The resistance of FNK/DCs to apoptosis induced by staurosporine. DCs were transfected with AdRGD-FNK or AdRGD-Luc at 50 MOI. After 48 h-cultivation, the transduced cells were cultured in the presence of 100 nM staurosporine for additional 24 h. The viability was assessed by MTT assay. Data are expressed as means ± SD of triplicate culture.

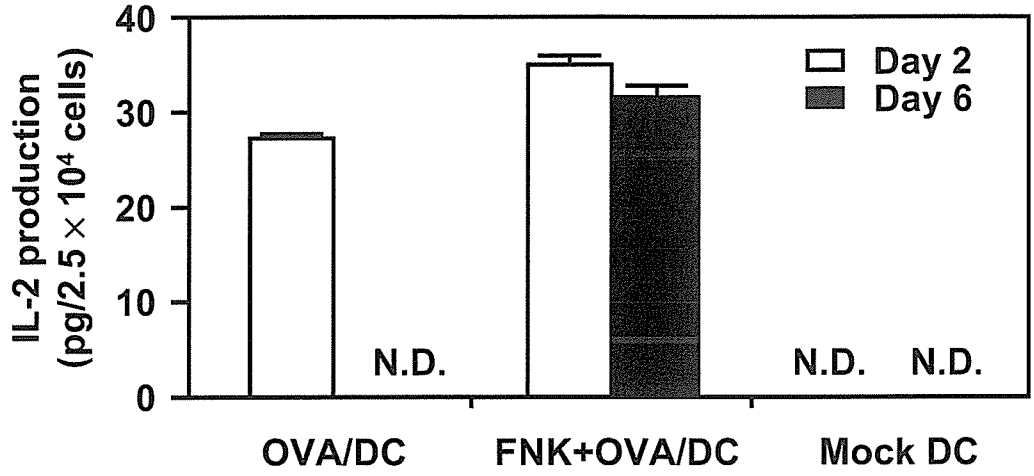

Fig. 88 Duration of antigen presentation in FNK/DCs. DCs were transfected with AdRGD-OVA alone (50 MOI) or the combination of AdRGD-OVA (50 MOI) and AdRGD-FNK (50 MOI) for 2 h. These transduced cells and mock DCs were cultured without cytokines and growth factors. On days 2 and 6, the levels of OVA-peptide presentation via MHC class I molecules on the transduced DCs were determined by bioassay using CD8-OVA1.3 cells. The data represents the means ± SD of three independent cultures. N.D.: IL-2 secreted from CD8-OVA1.3 cells was not detectable.

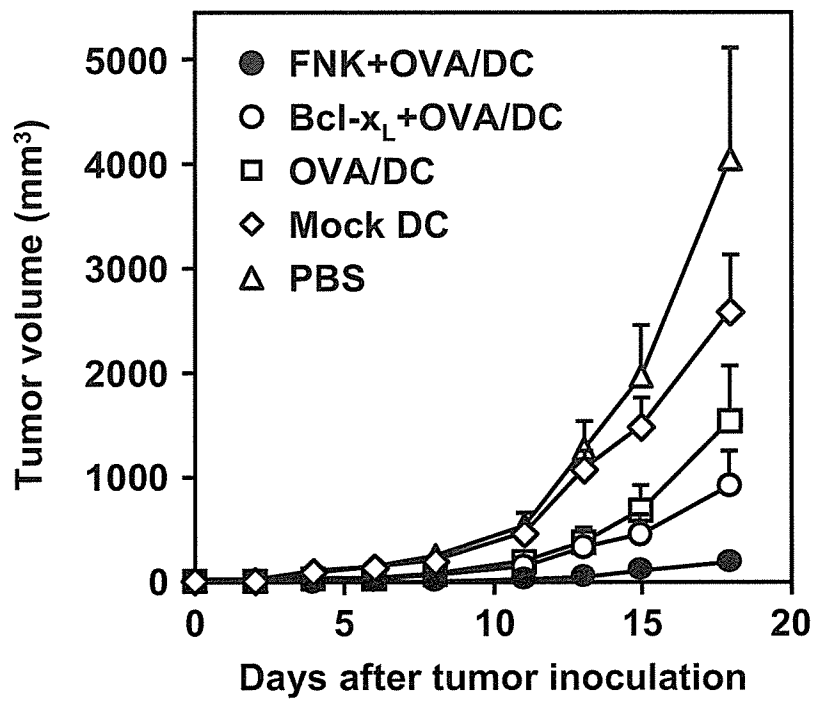

Fig. 89 Vaccine efficacy of DCs co-transduced with OVA gene and either Bcl-x_L or Bcl-xFNK gene against E.G7-OVA challenge. FNK+OVA/DCs, Bcl-x_L+OVA/DCs, and OVA/DCs were prepared using corresponding vectors at 25 MOI, and then cultures for 24 h. C57BL/6 mice were immunized by intradermal injection of transduced DCs into right flank at 5×10^4 cells. One week later, 10^6 E.G7-OVA cells were intradermaly inoculated into the left flank of these mice. The size of tumors was assessed using microcalipers three times per week. Each point represents the mean ± SE from 5-10mice.

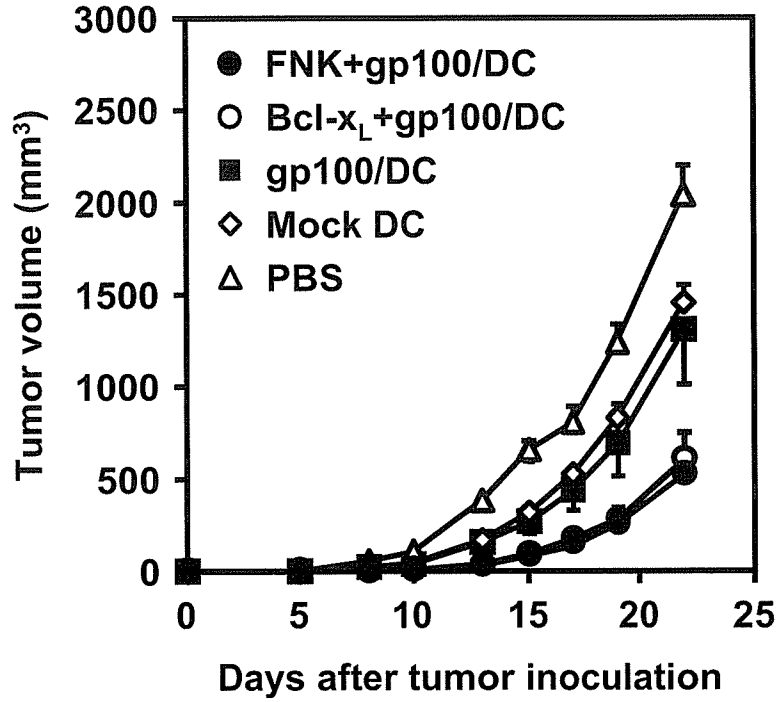

Fig. 90 Vaccine efficacy of DCs co-transduced with gp100 gene and either Bcl-x_L or Bcl-xFNK gene against B16BL6 challenge. FNK+gp100/DCs, Bcl-x_L+gp100/DCs, and gp100/DCs were prepared using corresponding vectors at 25 MOI, and then cultures for 24 h. C57BL/6 mice were immunized by intradermal injection of transduced DCs into right flank at 1.5×10^6 cells. One week later, 5×10^4 B16BL6 cells were intradermaly inoculated into the left flank of these mice. The size of tumors was assessed using microcalipers three times per week. Each point represents the mean ± SE from 5-10mice.

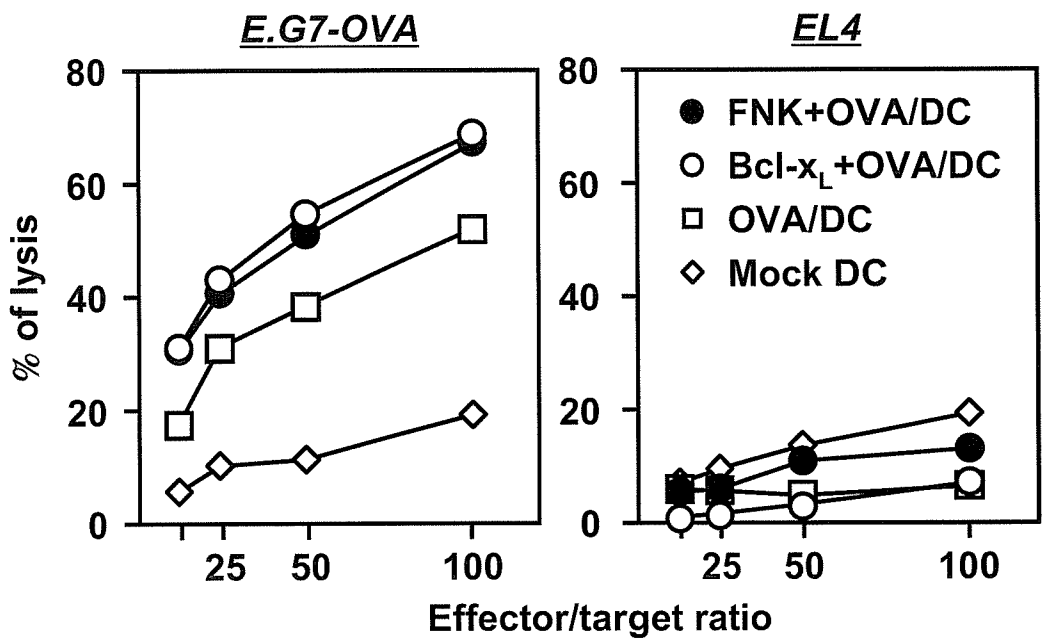

Fig. 91 OVA-specific CTL response in mice immunized with DCs cotransduced with OVA gene and either Bcl-x_L or Bcl-xFNK gene. FNK+OVA/DCs, Bcl-x_L+OVA/DCs, and OVA/DCs were prepared using corresponding vectors at 25 MOI, and then culture for 24 h. These transduced cells and mock DCs were vaccinated once intradermally into C57BL/6 mice at 2.5×10^4 cells. At 1 week after immunization, splenocytes were prepared from these mice, and were re-stimulated *in vitro* for 5 days with mitomycine C- inactivated E.G7-OVA cells. Cytolytic effects of re-stimulated splenocytes (effector cells) against E.G7-OVA or EL4 cells (target cells) were evaluated by ^{51}Cr-release assay.